Pacific Northwest
NATIONAL LABORATORY

Improvements to the $^{115g/115m}$Cd Nuclear Data

December 2021

Brian Archambault
Nicolas E. Uhnak
Bruce Pierson
Grant Spitler
Jane Estrada

U.S. DEPARTMENT OF
ENERGY

Improvements to the 115/115mCd Nuclear Data

December 2021

Brian Archambault
Nicolas E. Uhnak
Bruce Pierson
Grant Spitler
Jane Estrada

Executive Summary

Repeated measurements of the isotope ^{115m}Cd by Los Alamos National Laboratory (LANL), Pacific Northwest National Laboratory (PNNL), and Atomic Weapons Establishment (AWE) have revealed a consistent discrepancy between beta and gamma counting. This suggests that a significant disparity exists between the true value of the isotope's gamma-ray branching ratios and the values reported by the National Nuclear Data Center (NNDC).

Enriched ^{114}Cd was irradiated using thermal neutrons to produce a high-purity $^{115m/g}$Cd source for counting and analysis using traditional singles gamma-ray spectroscopy, liquid scintillation counting, gas-proportional counting, and analysis using the new Gamma-Alpha-Beta-Gamma (GABγ) and Gamma-Alpha-Beta Radio-Isotope EvaLuator (GABRIEL) coincidence detection systems. Using the D-T fusion generated neutrons, reduces the wait time required to let the short-lived ^{115}Cd ground state decay away by leveraging the 1:1 production ratio of the ground and metastable state of ^{115}Cd from the ^{115}In (n,p) reaction relative to the 10:1 production ratio of the ground and metastable isotopes of ^{115}Cd by thermal neutron capture on ^{114}Cd. However, the much higher flux in from the Washington State University TRIGA reactor is a more rapid method of production of $^{115m/g}$Cd but requires access to enriched ^{114}Cd.

High purity $^{115m/g}$Cd samples were analyzed on regular intervals over a period of 140-days. The activity of ^{115m}Cd measured by beta and gamma show a clear discrepancy using the current best known gamma-ray decay branching ratios.

Instrument	kBq/g	StDev	RSD
LSC	32.24	0.04	0.124%
GAB, 1601	32.80	0.10	0.305%
Gaby, LSC (ε_β~100%)	32.24	0.05	0.155%
Gaby, LSC-g (934 keV γ gate, ε_β~95.1%)	33.86	0.05	0.148%
GEA**	19.85	6.94(0.22&)	1.15%
**Using NNDC Branching Ratios (Blachot, Oct. 2012) & Standard deviation of 22 measurements conducted over 140 days			

Based on these observations and measurements, a set of new branching ratio recommendations have been produced using conventional counting techniques and the advanced GABγ and GABRIEL instruments.

^{115}Cd	GABγ			Conventional			GABRIEL		
Gamma	BR %	StdDev	RSD (%)	BR %	StdDev	RSD (%)	BR %	StdDev	RSD (%)
933.84	1.293	0.011	0.882	1.232	0.014	1.145	1.284	0.028	2.154
1290.59	0.566	0.005	0.938	0.534	0.008	1.498	0.574	0.011	1.992
484.47	0.194	0.002	0.786	0.187	0.004	2.139	0.181	0.003	1.627
1132.57	0.0535	0.0006	1.120	0.0514	0.0024	4.71	0.0548	0.002	3.059
158.03	0.0133	0.0002	1.578	0.0126	0.0015	11.9	0.0125	0.0003	2.469
1448.78	0.01047	0.00021	1.988	0.0098	0.0006	5.208	0.01068	0.00079	7.401
492.35				0.0081	0.0028	34.6	0.00565	0.00021	3.806
336.24							0.00353	0.00026	7.246

105.2	0.00266	0.00022	8.289			0.00337	0.00031	9.182
316.2	0.00389	0.00039	9.981			0.0034	0.0003	9.449
1418.24	0.000621	0.000016	2.600			0.000504	0.000029	5.675

Acknowledgments

Acronyms and Abbreviations

GEA: Gamma Emission Analysis

GABY: Gamma Alpha Beta Gamma

LSC: Liquid Scintillation Counting

Contents

Figures

Tables

1.0   Introduction & Background

Repeated measurements of the isotope ^{115m}Cd by Los Alamos National Laboratory (LANL), Pacific Northwest National Laboratory (PNNL), and Atomic Weapons Establishment (AWE) have revealed a consistent discrepancy between beta and gamma counting. This suggests that a significant disparity exists between the true value of the isotope's gamma-ray branching ratios and the values reported by the National Nuclear Data Center (NNDC). Further evidence supporting this theory is found in the relatively large uncertainties (~35%) given for the NNDC gamma-ray decay branching ratios of ^{115m}Cd (Blachot, Oct. 2012).

This isotope is an important fission product with strong sensitivity to the incident particle energy on a fissioning target nucleus. The neutron induced fission yield for ^{115m}Cd from ^{235}U fission increases by a factor of ~450 from thermal to D-T fusion neutron (~14 MeV) induced fission and also varies by as much as a factor of ~3 based on the fissioning actinide. Figure 1-1 and Figure 1-2 illustrate the energy and actinide dependence of the ^{115m}Cd fission product yield and ratio of the isomer and ground state as a function of neutron energy and actinide.
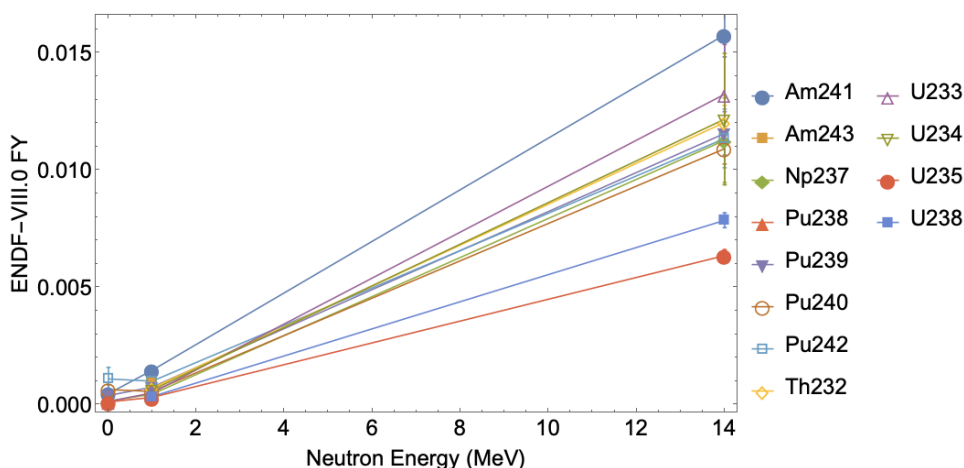
Figure 1-1, Plot of the ^{115m}Cd fission product yield as a function of incident neutron energy and fissioning actinide.

The intermediate life-time (~order days) and reasonably intense gamma-lines (~order percent) of ^{115m}Cd, make this isotope well suited to radio-tracer studies of elemental cadmium, neutron activation analysis of elemental cadmium concentrations, and is an important fission product to nuclear forensics. Unfortunately, the large gamma-ray branching ratio uncertainties preclude the use of high-resolution gamma-ray spectroscopy for accurate quantification. Quantification often requires tedious chemical separation, counting by beta, and yielding by mass spectrometric techniques.
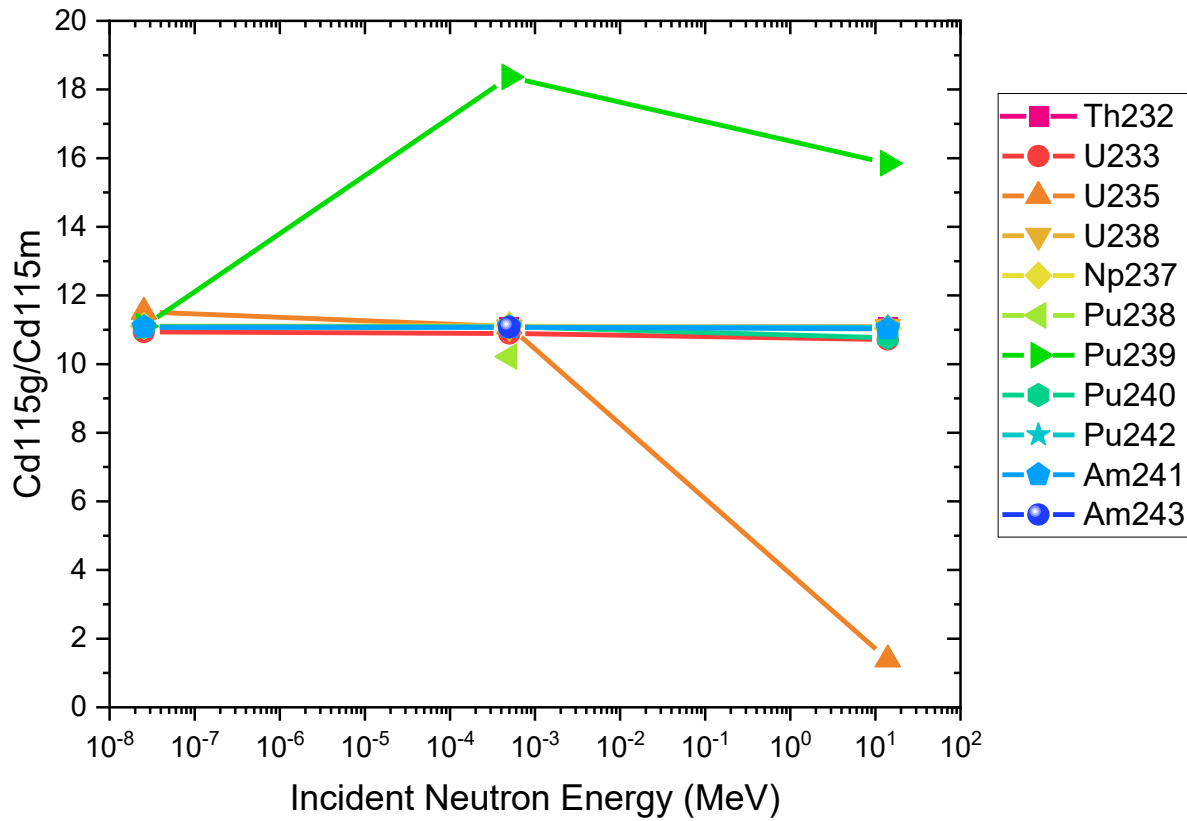
Figure 1-2, Fission product yield production ratio of the ground and isomer state of $^{115m/g}$Cd as a function of incident neutron energy and actinide.

Funding provided by the FBI for NTNF Improvements was used to investigate the discrepancy between beta and gamma quantification of ^{115m}Cd. This report summarizes the experiments, measurement results, and preliminary recommendations for more accurate ^{115m}Cd gamma-ray decay branching ratios.

2.0 Experiment

Two approaches were used to produce mono-isotopic sources of ^{115m}Cd. The first made use of the ^{115}In(n,p) $^{115m/g}$Cd proton knockout threshold reaction induced by a Thermo-Scientific accelerator driven deuterium-tritium fusion neutron source. The second used thermal neutron capture on an isotopically enriched ^{114}Cd target. The long lead time for receipt of enriched-^{114}Cd from the National Isotope Development Center (NIDC) and limited counting experience with mono-isotopic $^{115m/g}$Cd by beta and coincident spectroscopic techniques provided both time and need to experiment with alternative production methods of mono-isotopic ^{115m}Cd. The collective experience of producing mono-isotopic ^{115m}Cd sources using these two production methods are summarized in this section.

2.1 14 MeV Irradiations

Two Indium targets were irradiated on the 14 MeV neutron generator during two separate experiments. The 14 MeV neutron generator is located within the PNNL Low Scatter Facility. As a consequence of the target material being pure In, there was a need to remove the activated In from the produced Cd isotopes for counting using both liquid scintillation and gas proportional counting techniques. A high efficiency carrier free solvent extraction method was implemented at PNNL to isolate the Cd activation products in the organic phase from the bulk In target material. This methodology provides several key benefits including:

1. Reducing the In elemental load and quench in liquid scintillation counting, including gamma/beta coincidence spectroscopy via the recently developed Gamma-Alpha-Beta-Gamma (Gabɣ) instrument.

2. Reducing stable carrier material beta absorption in gas proportional counting.

3. Using the D-T fusion generated neutrons, reduces the wait time required to let the short-lived $^{115m/g}$Cd ground state decay away by leveraging the 1:1 production ratio of the ground and metastable state of $^{115m/g}$Cd from the ^{115}In(n,p) reaction relative to the 1:10 production ratio of the ground and metastable isotopes of $^{115m/g}$Cd by thermal neutron capture on ^{114}Cd.

2.1.1 Separation Method Development

Separation of In and Cd was achieved by taking advantage of the differences in their respective speciation in HCl acid, where Cd will form a polychloro anion at relatively low concentrations of HCl, while In will not (Martell, Smith, & Motekaitis, 2004). In the case of the 14 MeV irradiation of In, there were many orders of magnitude more In than Cd, therefore the separation needed to be highly effective.

Solutions of Cd and In were made using ICP-OES standard solutions in various ratios, 1:1, 10:1, and 1:10 Cd:In corresponding to 50 ppm Cd and In, 50 ppm Cd and 5 ppm In, and 5 ppm Cd and 50 ppm In, each in 0.1 M, 0.5, 1, 3, and 9 M HCl. The HCl used was Optima grade and diluted using de-ionized water with a resistance of 18 MΩ·cm; the Cd and In standard solutions were obtained from Inorganic Ventures in 2% HNO_3. All solutions were transposed to their final HCl concentrations for the experiment, thus minimizing the concentration of HNO_3.

A solution of 0.1 M Aliquat 336 (Chloride form, Alfa Aesar, 93%) in xylenes (Thermo Scientific 99%) was made by mass, chemical structures are shown in Figure 2-1. For the solvent extraction a volume ratio of 1:1 was used for the aqueous and organic phases, 2 mL of each phase was used. These solutions were shaken on a shaker table at 300 rpm for 30 minutes. The phases were separated by centrifuge at 3000 rpm, and 1 mL of the aqueous phase was diluted to 10 mL with 2% HNO_3 5% HCl. These samples were then analyzed by ICP-OES using a 5-point calibration curve with 2 ppm check standards.
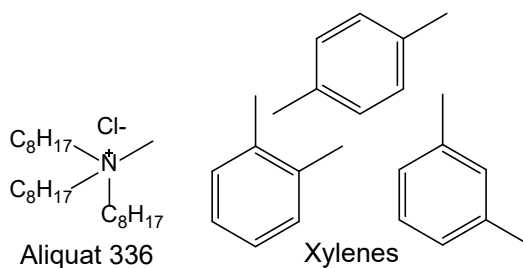
Figure 2-1: Chemical structures of Aliquat 336 and Xylenes

Significant reductions in quench can be achieved using pure organic liquid scintillation cocktail like UltimaGold F; however, the sample must be loaded onto a compatible organic to be compatible with pure UltimaGold F. This was a driving factor for extracting Cd in the xylene phase. Prior to the separation of the activated In, the compatibility of the extraction solvent was tested in several scintillation cocktails and mixtures. Figure 2-1 depicts the observed compatibility of UltimaGold F with xylene and Aliquat 336 (left), pure xylene (middle, left), hexane (middle right), and extracted Cd in xylene and Aliquat 336 (right). Though from Figure 2-2, it appears that the extraction solvent is miscible with the scintillation cocktail, once used in the extraction process there is enough extracted water that a pronounced cloudiness occurs. Given the incompatibility of the chemistry with pure organic cocktail, an alternative cocktail mix of 1:1 Ultima Gold F and AB scintillation cocktail was chosen for this work. Aqueous loading tables from the vendor along with past experience with this mixture suggest maximum aqueous loading of, at most, 10 uL/mL water-cocktail can be used with no effects on optical transparency of the samples.
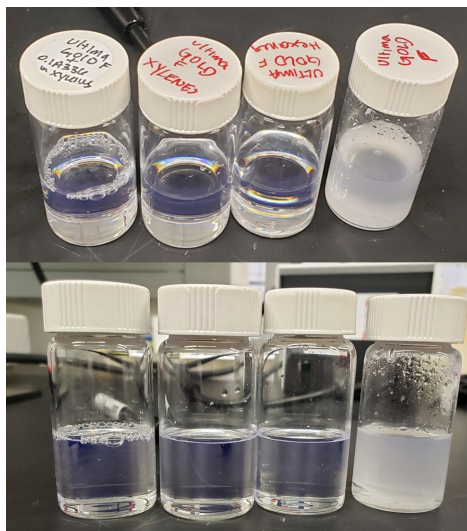
Figure 2-2. Comparison of 10 mL of Ultima Gold F with 1 mL of various solutions, going left to right those solutions are 0.1 Aliquot 336 in xylene, xylene, hexane, and 0.1 M HCl.

2.1.1.1 Separation of Irradiated In$_2$O$_3$

A 1.9297 g In$_2$O$_3$ target was irradiated for 4 hours on the 14 MeV generator as a loose powder inside of a glass scintillation vial. Following the irradiation, the sample was dissolved in a minimum volume of aqua regia (40 mL), producing a deep orange solution shown in Figure 2-3. This solution was then transposed to 0.1 M HCl, by evaporating to near dryness, adding 2 mL of concentrated HCl and repeating the process an additional two times. Finally, the solution was evaporated to near dryness, 2 mL of 0.1 M HCl was added, this was repeated twice more. After the final evaporation the solution was brought up to volume at 10 mL. Three separate 3 mL aliquots were taken for solvent extraction following a modified version of the process described in 2.1.1. The residual sample volume was diluted to 10 mL for GEA.

Figure 2-3, Irradiated indium oxide sample dissolving in aqua regia. The left image shows the actively dissolving sample, the right image shows the final aqua regia solution.

The extraction process is shown in Figure 2-4. Each of the three aliquots were contacted with 3 mL of 0.1 M Aliquat 336 extraction solvent, those aliquots were contacted twice more with fresh organic. The metal loaded extraction solvent was then combined and contacted with a fresh 9 mL volume of 0.1 M HCl to strip any extracted In, this In strip was repeated once more. Finally, the extraction solvent from each extraction were combined and evaporated to a 1 mL volume; 9 mL of the scintillation cocktail were added for analysis by the GABY coincidence detector. The In loaded aqueous samples were diluted to 10 mL and analyzed by GEA.
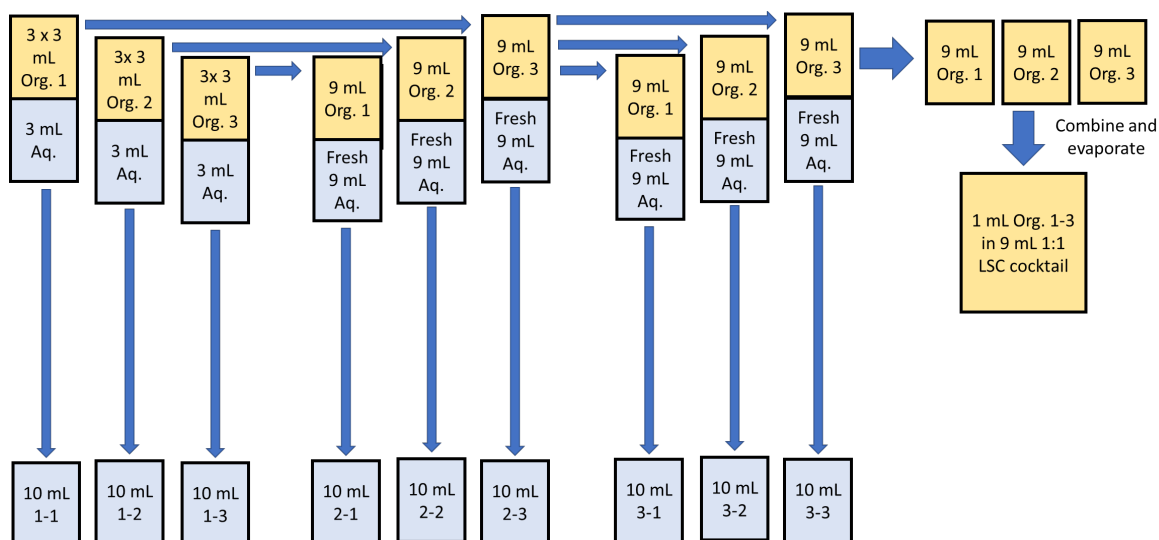
Figure 2-4. Solvent extraction process used for In_2O_3 irradiation sample.

2.1.2   Indium Metal

A 0.9741 g stack of In metal was irradiated for 6 hours on the face of the PNNL D-T generator on May 7th, 2021 starting at 7:42:20 to 13:52:32. A photo of the irradiation configuration is depicted in Figure 2-5. A neutron dosimetry package consisting of Al, Ni, Au, and Fe was also co-irradiated along with the In foil stack to verify the exposure intensity matched the expected output.

Figure 2-5. Image of In metal foil stack on the D-T Generator.

The target was disassembled, separating the Indium metal from the witness foil packet and aluminum foils. It was then dissolved in a beaker using 5 mL of concentrated HCl with the aid of 10 drops of concentrated HNO_3. Nitric acid was removed by evaporating the sample to dryness, the residue remaining was then dissolved in concentrated HCl, this process was repeated a final time bringing the final sample up in 10 mL of 0.1 M HCl.

Of the 10 mL, 9 mL were used for purification of Cd using solvent extraction and 1 mL for direct gamma counting. The results of this analysis were used as the starting activity of each isotope in solution. The solvent extraction of Cd proceeded according to the scheme shown in Figure 2-6. The 9 mL fraction was contacted with 9 mL 0.1 M Aliquat 336 in xylenes as mentioned previously and the aqueous phase eluted off the organic. The organic phase was then

contacted with clean 9 mL 0.1 M HCl four additional times, each eluant was counted using gamma spectroscopy. The final 9 mL extraction solvent containing purified Cd was evaporated to a total volume of one mL before adding 9 mL of 1:1 Ultima Gold AB:F cocktail for analysis by the GABY detector.
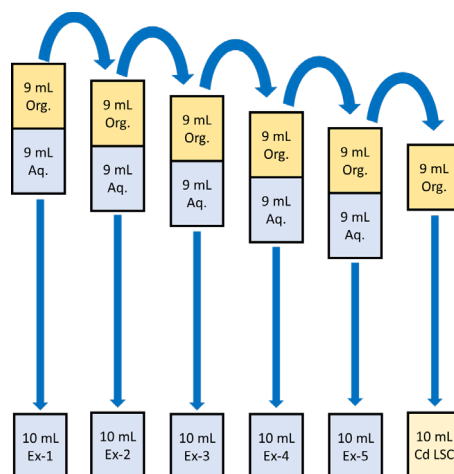
Figure 2-6. Solvent extraction process used to separate the 14 MeV neutron irradiated In foil.

2.2 Thermal Irradiations

Thermal irradiations used an isotopically enriched Cd metal source and relied on production by thermal neutron absorption in ^{114}Cd (n,γ) $^{115m/g}$Cd. Cadmium isotopics of the sample are provided in Table 2-2. Unlike the 14 MeV irradiations, chemistry is not necessary to produce a pure ^{115}Cd sample though can be used to remove impurities from decay products or otherwise.

The solvent extraction methods developed can also be used to separate and study the short-lived ^{115m}In isomer following decay of $^{115m/g}$Cd.

Table 2-1. Isotopic composition of ^{114}Cd enriched Cd metal.

Isotope	Percent composition
^{106}Cd	<0.01
^{108}Cd	<0.01
^{110}Cd	0.0860 ± 0.003
^{111}Cd	0.1830 ± 0.005
^{112}Cd	0.37 ± 0.01
^{113}Cd	0.48 ± 0.01
^{114}Cd	98.69 ± 0.02
^{116}Cd	0.178 ± 0.05

2.2.1 Cadmium Nitrate

A Cd salt was irradiated for 8 hours on June 4th, 2021 from 8:46:49 PST to 16:46:51 in the Washington State University TRIGA reactor at position E9. The $Cd(NO_3)_2$ salt used for the thermal irradiation was made by dissolving 22.696 mg of Cd metal in 0.5 mL of 0.1 M HNO_3 in the irradiation vial, the solution was then evaporated leaving the $Cd(NO_3)_2$ residue on the

bottom of the plastic ½ dram vial and brought up in 1 mL of 0.1 M HCl. The sample was prepared for gamma spectroscopy analysis by adding 9 mL of 1:1 UltimaGold F:AB cocktail. The measured activity of the metastable and ground state of $^{115m/g}$Cd at the end of exposure is provided in Table 2-2.

Table 2-2, Measured end of bombardment activities.

Isomer	Activity (Bq)	1σ %
^{115g}Cd	7.82e6	+/-2%
^{115m}Cd	3.50e4	+/-35%

Because of the limited availability at the Washington State University TRIGA reactor, the irradiation was shorter than necessary to produce all the sample fractions needed to perform traditional-LSC, gas proportional, traditional-singles gamma spectroscopy, and Gaby counting in duplicate over the 120-day period needed to carefully follow the decay of the isotope. This first experiment was used as a test experiment to determine the production and recovery of the irradiated sample material and determine whether any significant activation impurities would be generated. Sample impurities would inhibit the accuracy of pure beta counting without chemical purification.

Unfortunately, the Gaby instrument suffered a vacuum failure in one of the HPGe detectors early on during counting and had to be sent out for repair. Only a limited dataset was acquired from this sample, but no significant long-lived activation impurities were observed. Table 2-2 presents measured activities of activation product impurities. The ^{24}Na and ^{140}La activities were expected and considered impurities in the quartz rather than the Cd sample itself. This was later confirmed in the following section.

Table 2-3, Measured activities of two prominent impurities in the screening count.

Isomer	Activity (Bq)	1σ %
^{24}Na	1.07e4	+/-10%
^{140}La	56	+/-25%

2.2.2   Cadmium Metal

For the long thermal irradiation an ampoule was double sealed containing 12.691 mg of 98.6% ^{114}Cd. Figure 2-7 depicts the fluence monitor package and ^{114}Cd sample sealed in quartz before irradiation. The ampoule was irradiated according to the times and dates described in Table 2-3. Each irradiation was followed by a cooling period, this cooling period allowed for a portion of the ^{115g}Cd produced to decay away while continuing to integrate the total activity of ^{115m}Cd.
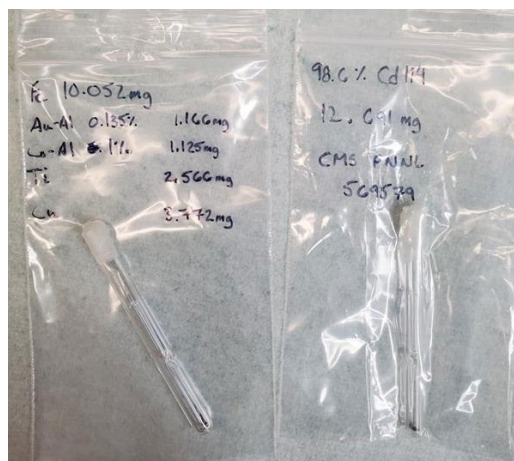
Figure 2-7, Photos of the fluence monitor set and 114Cd sample sealed in quartz.

Table 2-4. Irradiation and cooling times for Cd metal target.

Date	Time in	Time out	MW hours
6/25/21	7:59:23	9:58:00	1.98
6/25/21	10:50:50	16:52:17	6.02
6/27/21	9:31:44	17:31:44	8.00
6/28/21	8:51:09	12:02:05	3.18
6/28/21	12:43:20	16:55:24	4.20
6/29/21	8:57:40	16:57:40	8.00
6/30/21	8:32:47	16:57:47	8.42
7/1/21	8:49:33	16:56:32	8.12
7/2/21	8:41:46	16:46:37	8.08

The irradiated Cd was first screened using a high-purity germanium detector, T, at several feet upon receipt of the sample. The screening activity of $^{115m/g}$Cd at end-of-bombardment is provided in Table 2-2.

Table 2-5, Measured end of bombardment activities of the ^{114}Cd metal sample.

Isomer	Activity (Bq/g)	Activity (Bq)	1σ %
^{115g}Cd	6.76e8	8.58e6	+/-2%
^{115m}Cd	6.91e6	8.77e4	+/-35%

After screening the ^{114}Cd ampoule was placed into a custom catch for quartz ampoule destruction and crushed using a lead brick. The sample including the quartz was transferred to a clean 50 mL glass beaker. Rinses of 2 M HNO_3 were used to clean the inside of the catch, rinsing into the glass beaker. The beaker was moved to a hot plate where the solution was heated to dissolve the metal. The solution was then separated from the quartz shards and transferred to a new 50 mL glass beaker. Five 1 mL rinses were used to recover any remaining Cd solution from the quartz shards into the new 50 mL glass beaker. Finally, the glass beaker was transferred to the hot plate and brought to near dryness. The dissolved solid was brought up in 2 mL of 0.2 M HNO_3 and transferred to a tarred plastic scintillation vial, along with three 1

mL rinses. The final mass of the stock solution was 4.8018 grams. For convenience the stock solution will be referred to as solution "A."

The long WSU thermal irradiation of ^{114}Cd produced the greatest quantity of both $^{115m/g}$Cd. The dissolved sample was separated into multiple samples for detailed radiometric analysis using conventional LSC, gas proportional, and combined gamma-alpha-beta-gamma coincidence counting using two custom instruments developed at PNNL. Table 2-4 lists the samples and analysis methods for the sample fractions generated from the dissolved ^{114}Cd sample.

The Gaby (**G**amma-**A**lpha-**B**eta-**γ**) detector consists of a small liquid scintillation counter located between two Ortec GMX n-type coaxial HPGe detectors. Data are acquired from two photo-multiplier tubes and the two HPGe detectors simultaneously using a common clock reference. The data must be acquired time-synchronously to be used to reconstruct coincident events between detectors following data acquisition. Figure 2-7 depicts the Gaby detector with a standard blank set in the counting position.

Table 2-6, Sample fractions and dilutions prepared for assay of ^{115m}Cd.

Sample ID	Assay Technique	Mass of A (g)	Activity (Bq)
GEA 1	Gamma Spectroscopy	0.4849	8800
GEA 2 (CNAAPS)	Gamma Spectroscopy	0.4843	8800
LSC	Gamma Spectroscopy & Liquid Scintillation Counting	0.4835	8800
GABY	GABY	4.84E-01	8055.313
GAB1	Gas Proportional Counting	2.10E-03	34.9894
GAB2	Gas Proportional Counting	2.09E-03	34.785
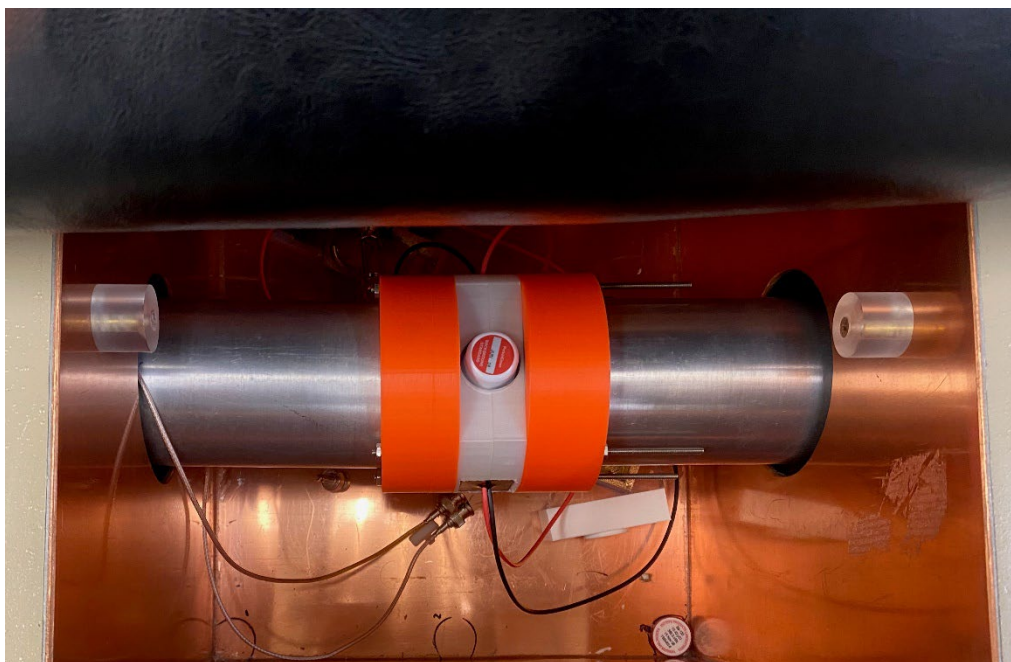
Figure 2-8. Photo of the Gaby detector.

This provides improved detection sensitivity for select analytes using alpha and beta events observed in the LSC as both a coincidence gate and veto. Operationally, data are acquired in list-mode and post-processed following the count into a suite of custom spectra. This set of spectra includes:

1. Gamma spectra from each HPGe detector with no gating
2. Gamma spectra from each HPGe using the LSC as a veto
3. Gamma spectra from each HPGe containing events in coincidence with the LSC

The spectra are analyzed using custom analysis utilities based on CERN's ROOT data analysis framework (Brun & Rademakers, 1997).

Data were acquired periodically using Gaby starting at 17 days following the end of bombardment for a total measurement time of 19 days over a period of 39.6 days. Unfortunately, only the first 24 hours of data collected on Gaby utilized both HPGe detectors. The second HPGe for Gaby was returned before sample receipt in marginal working condition and failed shortly after returning the instrument back to service.

Further experimentation continued with the operation of the LSC and one HPGe detector. A second instrument, termed Gabriel (**G**amma-**A**lpha-**B**eta **R**adio**I**sotope **E**va**L**uator) was later commissioned in September 2021 as a replacement for Gaby and was utilized for subsequent analysis. The Gabriel detector consists of a small profile liquid scintillation counter (LSC) and one Ortec "PROFILE" GEM-S p-type coaxial HPGe detector and one Ortec "PROFILE" GEM-SP p-type semi-planar HPGe detector (both with carbon fiber end windows) which acquired data time-synchronously. Data were acquired from the two photo-multiplier tubes in the LSC counter of Gaby in list-mode using a CAEN DT5730 digitizer with pulse shape discrimination firmware. Data from the HPGe detectors were acquired using a CAEN DT5781 operating with pulse height analysis firmware. These were time-synchronized using a CAEN DT4700 external clock. As configured, the Gabriel detector exhibits superior detection efficiencies at low energies, better energy resolution, and lower noise when compared to its predecessor Gaby. Data were acquired periodically using Gabriel starting at 87 days following the end of the irradiation for a total measurement time of 15.7 days over a period of 51.8 days.

3.0 Results

This effort included product, chemical processing, and radiation spectroscopy analysis of sample data. This section reviews the efficacy of the chemical processing methods and measured branching ratios of ^{115m}Cd

3.1 Indium Cadmium Separation Method Development

The efficacy of the solvent extraction separation of In and Cd was calculated using the following formulas. Distribution ratio (D) is the ratio of the concentration of the analyte in the organic phase and aqueous phase, due to the method of analysis, mass balance of metal allows for a modification to account for analysis of only an aqueous phase. Where the concentration of the analyte in the organic phase becomes the difference between the pre-extraction (M_i) and post extraction analyte (M_f) concentration. This is shown in Equation 1. For discussion below the use of %E or extraction efficiency is used, defined below, using the distribution ratio determined from the analysis, as shown in Equation 2.

$$D = \frac{[M]_{org}}{[M]_{aq}} = \frac{[M_i - M_f]}{[M_f]} \tag{1}$$

$$\%E = \frac{D \times 100}{D + 1} \tag{2}$$
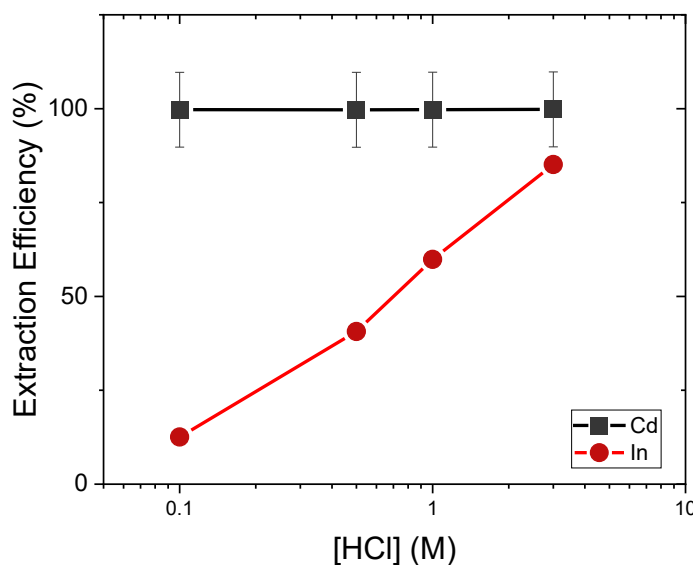
Figure 3-1. Extraction efficiency of Cd and In as a function of the log of the HCl concentration for the 1:10 ratio of Cd to In. Values are the result of triplicate samples, uncertainty in the In values are 1 σ. Uncertainty in the Cd values are an assumed 10% due to the quantitative nature of the extraction.

Due to the effectiveness of the extraction (~100%), there is an assumed 10% uncertainty in the %E. This is due to a large difference in D arising from small differences in the organic phase analyte concentration which precludes the measurement by difference.

Separation was easily achieved for the Cd and the In using the solvent extraction method, which has the added benefit of the Cd being retained in an organic phase, ideal for liquid scintillation counting. The results of the solvent extraction of the 1:10 Cd:In is shown in Figure 3-1. At all examined conditions there was quantitative extraction of Cd, while there is a logarithmic relationship between E% and the log[HCl]. This relationship between the In extraction and the concentration of the HCl is a direct consequence of the speciation of In in those conditions. All other Cd:In ratios examined had nearly identical behavior to the presented work. Due to the stable nature of these examinations the concentrations used for the Cd are significantly higher than would be expected from the In irradiation on the 14 MeV generator.

Though there was ~15% of the In extracted in the 0.1 M HCl, this was selected as the concentration moving forward, allowing there to be sufficient concentrations of Cl to overcome any possible thermodynamic issues when moving forward to larger masses of In, like those used in the 14 MeV irradiations. Rather than depending on the single extraction to provide an adequate separation multiple contacts were used. Subsequent extractions from the organic entailed contacting the Cd metal loaded organic solvent (0.1M Aliquat 336 in Xylenes) with a fresh 0.1 M HCl solution, stripping the remaining In from the Cd. As the number of these strips increased the purity of the extracted Cd also increased.

3.2   Irradiated Indium Oxide Separation and Analysis

Isotope	Primary Gamma Energy Analyzed	Bq/g ± 1σ%	
^{112g}In	617	2.8×10^6	± 28.2%
^{112m}In	156	2.70×10^5	± 1.2%
^{113m}In	392	4.81×10^3	± 0.8%
^{114m}In	190	1.89×10^3	± 4.7%
^{115g}Cd	528	148	± 1.2%
^{115m}In	336	4.38×10^4	± 2.0%
^{116m}In	1294	1.62×10^5	± 1.2%

Table 3-1. Activity of major isotopes in irradiated In_2O_3 sample. Values are in Bq/g of sample with 1σ uncertainty.

The activity of the radioisotopes contained in the solution following irradiation and dissolution of the In_2O_3 target are presented in Table 2-1. Multiple nuclear reactions occurred on this sample, as can be seen in the variety of In activation products present post-irradiation. The Cd was loaded into the organic and subsequently purified with additional In extractions. The percent of In remaining in the aqueous phase was calculated from GEA analysis of each subsequent In extraction using ^{114m}In as a radiotracer. The total activity of ^{114m}In the starting solution and the final activity in each of the post extraction/contact solutions were used to estimate how much In remained in the organic Cd fraction. The percent of the In (^{114m}In) extracted following three purifications of the organic Cd fraction are shown Figure 3-2. Notably there was no detectable Cd activity. The final Gaby sample showed 0.74% of the initial ^{114m}In remaining with 100% of the $^{115m/g}$Cd recovered. The separation proceeded with >80% of the extracted In activity being stripped with each subsequent contact.
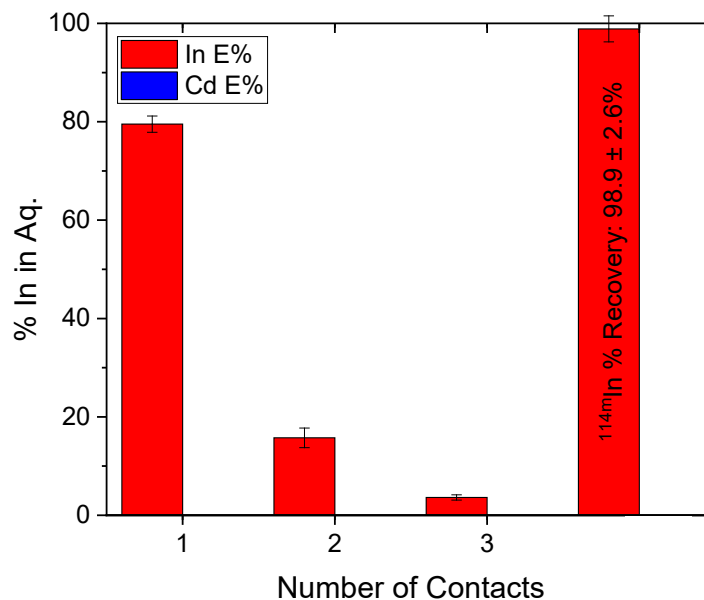
Figure 3-2. Percent of [114m]In remaining in each aqueous phase after contact with the extraction solvent. Contact 1 is the initial extraction, contact 2 and 3 are the In strip contacts. All values are the average of triplicate samples reported with 1σ in that value. The sum of the activity is presented as the sum of the three contacts.

3.3 Irradiated Indium Metal Foil Separation and Analysis

The activity of isotopes of interest in the irradiated In metal foil are shown in Table 3-2. Several activated indium isotopes were studied as part of this second trial. The short-lived [116m]In and [115m]In isotopes along with the long-lived [114m]In were used as redundant internal In tracers for the analysis of the solvent extraction results of the second 14 MeV activation experiment. The 528 keV gamma-line from [115g]Cd was used to quantify this isotope in the extractant solutions and used as a tracer of the Cd concentration. The statistical accuracy of the [115g]Cd activity in the bulk dissolved solution was relatively low due to the large Compton continuum under the 528 keV gamma-line produced by the short-lived In isotopes.

Table 3-2. Activity of Isotopes of Interest in 14 MeV irradiated In metal foil.

Isotope	Bq/g ± 1σ%	
[114m]In	2.01×10^4	± 3.6
[115m]Cd	1.59×10^3	± 13.9%
[115m]In	4.18×10^5	± 0.7%
[116m]In	1.01×10^6	± 2.6%

The solvent extraction method (Figure 2-4) used produced a highly pure Cd fraction containing little of the initial [114m]In activity. The previous experiments showed quantitative extraction of Cd into the organic solvent and only ~10-15% of the total In. In this experiment quantitative separation of Cd from In was not observed as shown in Figure 3-3. Sample Ex-1 shows ~80% recovery of all three In isotopes as expected with ~2% of the Cd. This was unexpected and remains unclear what may have produced this difference. The unexpected recovery of Cd in Ex-

5 may have been driven thermodynamically by the absence of In in the sample relative to Cd. Nevertheless, the final Cd fraction contained 92.5% of the initial ^{115g}Cd activity, with 0.13% of the initial ^{114m}In activity.
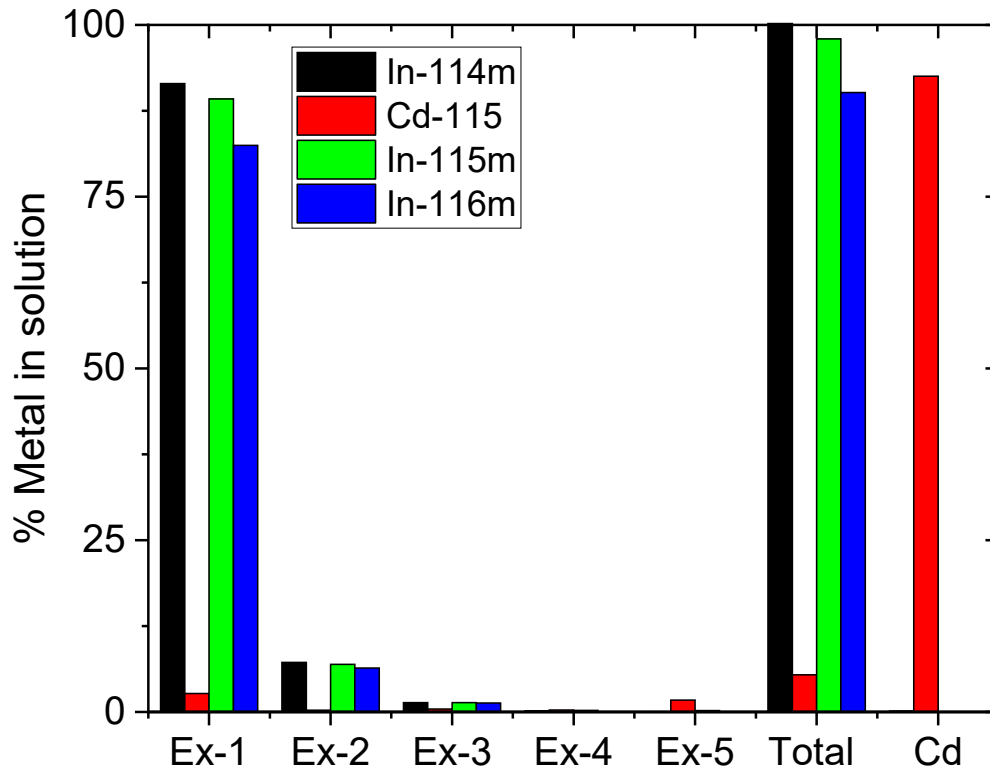
Figure 3-3. Percent of metal remaining in each fraction, extracting Cd from irradiated In metal target. Ex designation denotes the percent remaining in the aqueous phase, Ex-1 is the initial extraction, Ex-2-5 are In strip steps.

3.4 Determination of γ-ray BRs for ^{115m}Cd

A total of 7×10^7 coincident β-γ counts were recorded by Gabγ and 2.7×10^7 coincident β-γ counts were recorded by Gabriel over the course of the measurement campaign. The time difference between the β and γ signals for each instrument are shown in Figure 3-4.
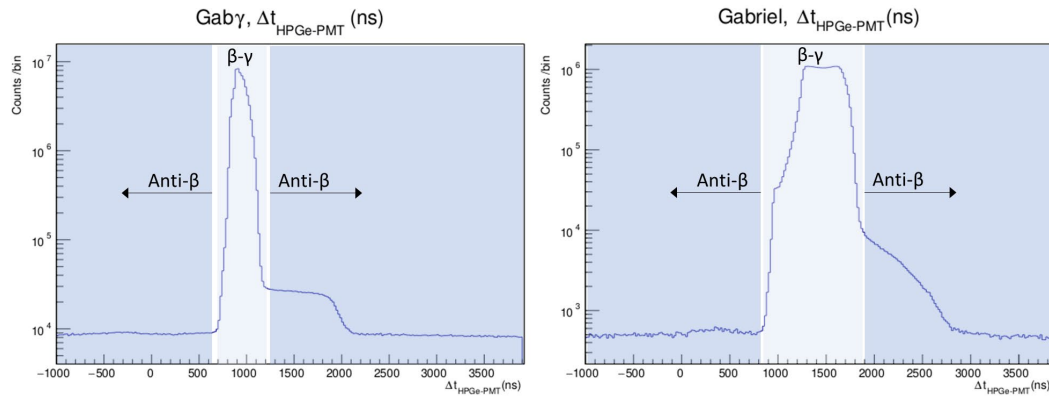
Figure 3-4. Measured time-difference spectrum for beta-gamma coincidences as measured with Gaby and Gabriel.

The central peaks in each spectrum are attributed to true β-γ coincidence events, while the regions above and below the central peaks are attributed to random and uncorrelated coincidences. Sources of uncorrelated coincidences may be due to random accidental coincidences with after-pulsing in the PMTs, background sources, or gamma emissions due to isomeric transition or internal conversion. The corresponding gamma, beta-gamma, and anti-beta gamma spectra as measured by Gabriel are presented in Figure 3-5.
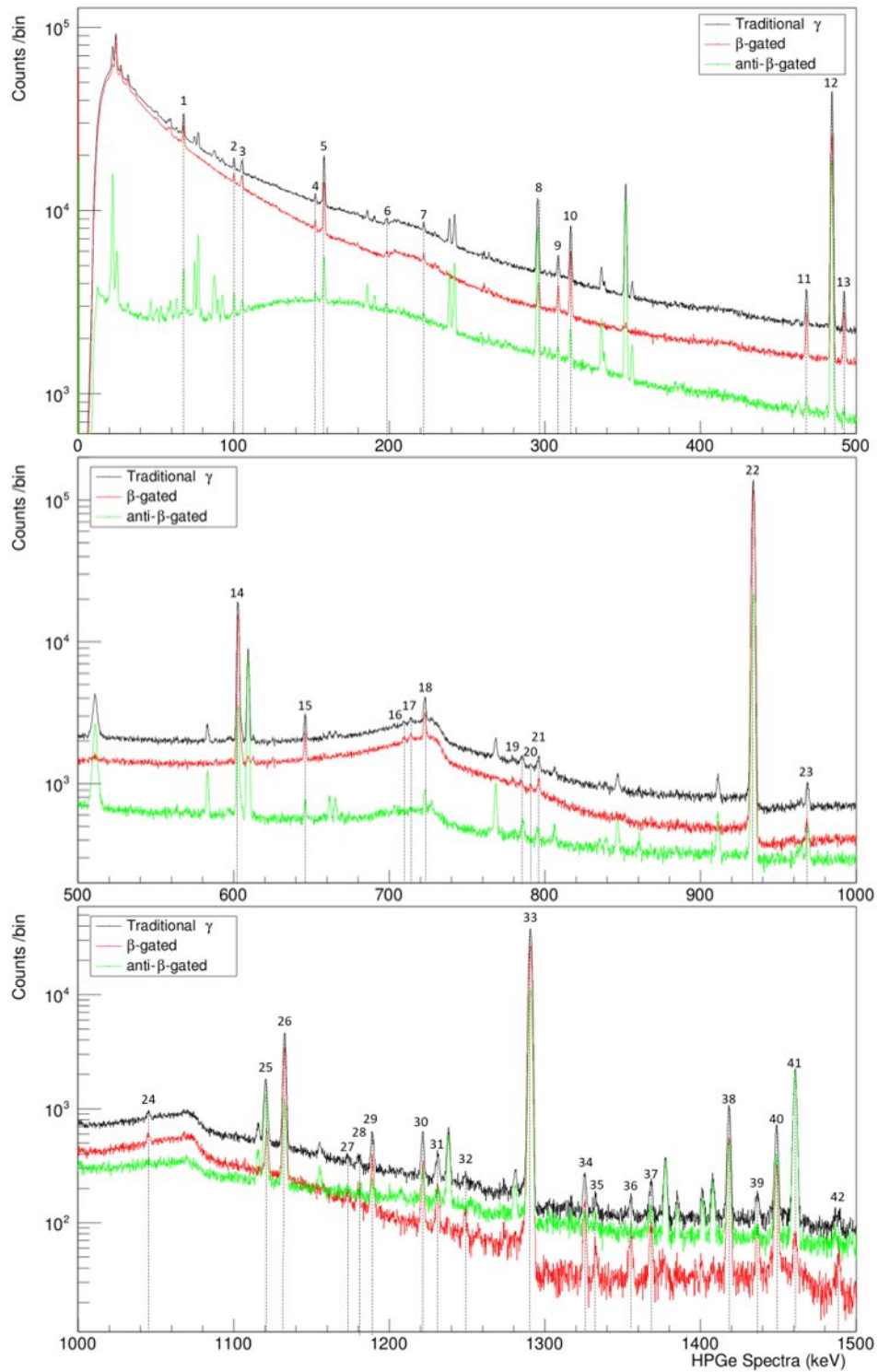
Figure 3-5. Measured and annotated Gabriel gamma, beta-gated gamma, and anti-beta-gated gamma spectra for GABY3 sample.

Significant β-γ coincidence peaks were identified and attributed primarily to the presence of ^{115g}Cd or ^{115m}Cd, along with the presence of several minor impurities including ^{124}Sb, ^{182}Ta, ^{192}Ir, and ^{60}Co as shown in Table 3-3. These impurities contribute to the decays measured in the liquid scintillation cocktail in Gabγ and Gabriel but did not affect the results of the final absolute γ-ray branching ratios. The massic activity for each major impurity was calculated and decay corrected using the Bateman equation to the concentrations present at the end of the sample irradiation. Spectra were anlayzed using a custom ROOT (Rademakers & Brun, 1997) peak-fitting tools (Pierson & Archambault, TListSpectrum, 2022). Their massic activities and the gamma lines used to determine them are shown in Table 3-4 for ^{124}Sb, ^{182}Ta and ^{192}Ir. Massic activity of the ^{60}Co was not determined since its primary gamma line at 1173.5 keV was more than ×100 times weaker than the gamma lines from either ^{192}Ir or ^{182}Ta.

Table 3-3. Identification of gamma peaks of interest labeled by their beta decay parent.

| Peak	Identification	Note:	Peak	Identification	Note:
1	67.75 keV, ^{182}Ta	Impurity	22	934 keV, ^{115m}Cd	
2	100.27 keV, ^{182}Ta	Impurity	23	968 keV, ^{124}Sb	Impurity
3	105.2 keV, ^{115m}Cd		24	1045 keV, ^{124}Sb	Impurity
4	152.6 keV, ^{182}Ta	Impurity	25	1121 keV, ^{182}Ta	Interfered
5	158.0 keV, ^{115m}Cd		26	1133 keV, ^{115m}Cd	
6	198.37 keV, ^{182}Ta	Impurity	27	1173.5 keV, ^{60}Co	Impurity
7	222.2 keV, ^{182}Ta	Impurity	28	1180.8 keV, ^{182}Ta	
8	296.0 keV, ^{192}Ir	295.2 keV, Pb-214	29	1189 keV, ^{182}Ta	Impurity
9	308.7 keV, ^{192}Ir	Impurity	30	1222 keV, ^{182}Ta	Impurity
10	316.7 keV, ^{115m}Cd	316.5 keV, Ir-192	31	1232 keV, ^{182}Ta	Impurity
11	468.3 keV, ^{192}Ir	Impurity	32	1249 keV, ^{228}Ac	Background
12	484.7 keV^{115m}Cd		33	1291 keV, ^{115m}Cd	
13	492.5 keV, ^{115m}Cd		34	1326 keV, ^{124}Sb	Impurity
14	602.7 keV, ^{124}Sb	604.4 keV, Ir-192	35	1332.6 keV, ^{60}Co	Impurity
15	645.9 keV, ^{124}Sb	Impurity	36	1355 keV, ^{124}Sb	Impurity
16	709 keV, ^{124}Sb	Impurity	37	1368 keV, ^{124}Sb	Impurity
17	714 keV, ^{124}Sb	Impurity	38	1418 keV, ^{115m}Cd	
18	723 keV, ^{124}Sb	Impurity	39	1437 keV, ^{124}Sb	Impurity
19	785 keV, ^{192}Ir Sum	468 keV + 316.5 keV	40	1445 keV, ^{124}Sb	Impurity
20	791 keV, ^{124}Sb	Impurity	41	1461 keV, ^{40}K	Background
21	796 keV, ^{228}Ac	Background	42	1489 keV, ^{124}Sb	Impurity

Table 3-4. Quantification of impurities in GABY 3 sample as measured by Gabriel used for BR determination and interference corrections.

Impurity	Bq/g	stdev	RSD	Notes
^{124}Sb	21.7	0.2	0.8%	1691 and 723 keV lines
^{182}Ta	2.81	0.09	3.2%	68, 1189, and 1221 keV lines
^{192}Ir	2.14	0.11	5.1%	468.1 and 308.5 keV lines

It is important to note, that although several impurities were present in the GABY sample, the concentration of the largest impurity, ^{124}Sb, was <0.1% of the total ^{115m}Cd activity. Additionally, the presence of ^{192}Ir is important as it has a strong gamma line at 316.5 keV with an absolute gamma intensity of 82.86% which interferes with the relatively weak 316.2 keV gamma line from ^{115m}Cd with an absolute intensity of 0.0025% (Blachot, Oct. 2012). This doublet is unresolved by the HPGe detectors in both the Gabγ and Gabriel instruments.

A total of 1.4×10^{10} counts were recorded by the LSC in Gabγ over a total measurement time of 19 days spanning a period of 39.6 days. Stability of the LSC cocktail was tracked throughout the measurement period using the ratio of the full energy peak for the 934 keV line in the gamma spectrum with full energy peak in the beta-gamma coincidence spectrum. The corresponding beta efficiency was measured as 95.1(3)% and is shown in Figure 3-6.
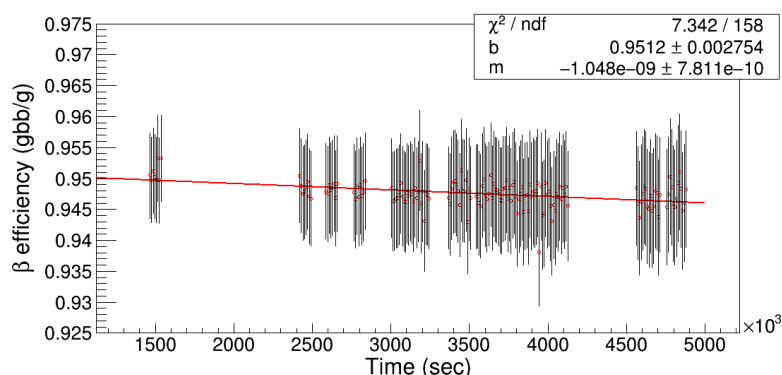
Figure 3-6. Measured GABY3 sample β efficiency using 934 keV γ gate throughout counting period.

It is important to note that the measured beta efficiency using the 934 keV gamma gate corresponds to an endpoint beta energy of 697 keV which accounts for only 3% of the total beta emission spectrum. The other 97% of beta decays feed the ground state of Indium directly with a much higher 1620 keV endpoint beta energy. This effect is graphically illustrated in Figure 3-7, in which the total beta emission spectrum corresponding to the decay of ^{115g}Cd, ^{115m}Cd, ^{115m}Cd in coincidence with 934 keV gamma emission, and a Sr/Y-90 LSC standard calibration source are shown (Mougeot, 2019).
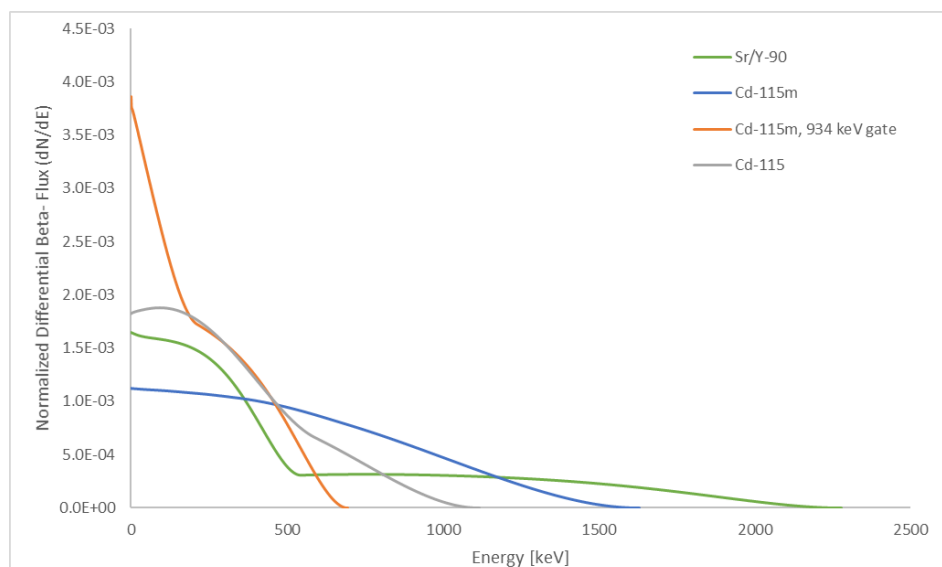
Figure 3-7. Normalized differential β flux for Sr/Y-90 calibration standard, ^{115g}Cd, ^{115m}Cd, and ^{115m}Cd gated in coincidence with 934 keV gamma.

A rigorous analysis of the LSC data from Gaby was conducted and is summarized in Figure 3-8. A dual (accounting for ^{115g}Cd and ^{115m}Cd) exponential curve was fit to 54,720 30-second counting intervals using least squares fitting and is shown in Figure 3-8a. The fitting equation used included corrections for a beta efficiency stability of 0.3%, static beta detection efficiencies of 95% and 100% for ^{115g}Cd and ^{115m}Cd, respectively, a fixed ^{115g}Cd half-life of 53.46(5) hr., a background rate of 1.73 cps, and the paralyzable dead-time correction model defined in Equation (3).

$$C_{out} = C_{in}e^{-C_{in}\tau} \tag{3}$$

where
C_{out} = measured detection rate
C_{in} = true detection rate
τ = dead-time per detection event.

The resultant fit yielded massic activities of 32,120(11) kBq/g of ^{115g}Cd and 32.24(5) kBq/g of ^{115m}Cd at the end of irradiation and a ^{115m}Cd half-life of 44.44(4) days which agrees within 1 standard deviation of the published NNDC half-life of 44.56(24) days. This half-life estimate was also compared to an estimate derived from fitting a Lorentzian peak to a histogram of two-point half-life measurements sampled from all 54,720 points (Figure 3-8c). The normalized residual was also binned and fit using a gaussian to test normality of the data as shown in Figure 3-8b. The residuals, forward running half-life and uncertainty budget as a function of time are also provided in Figure 3-8d-f.

Figure 3-8. Detailed analysis of LSC measurements with Gaby used to determine massic activities of ^{115g}Cd and ^{115m}Cd as well as verify the ^{115m}Cd half-life.

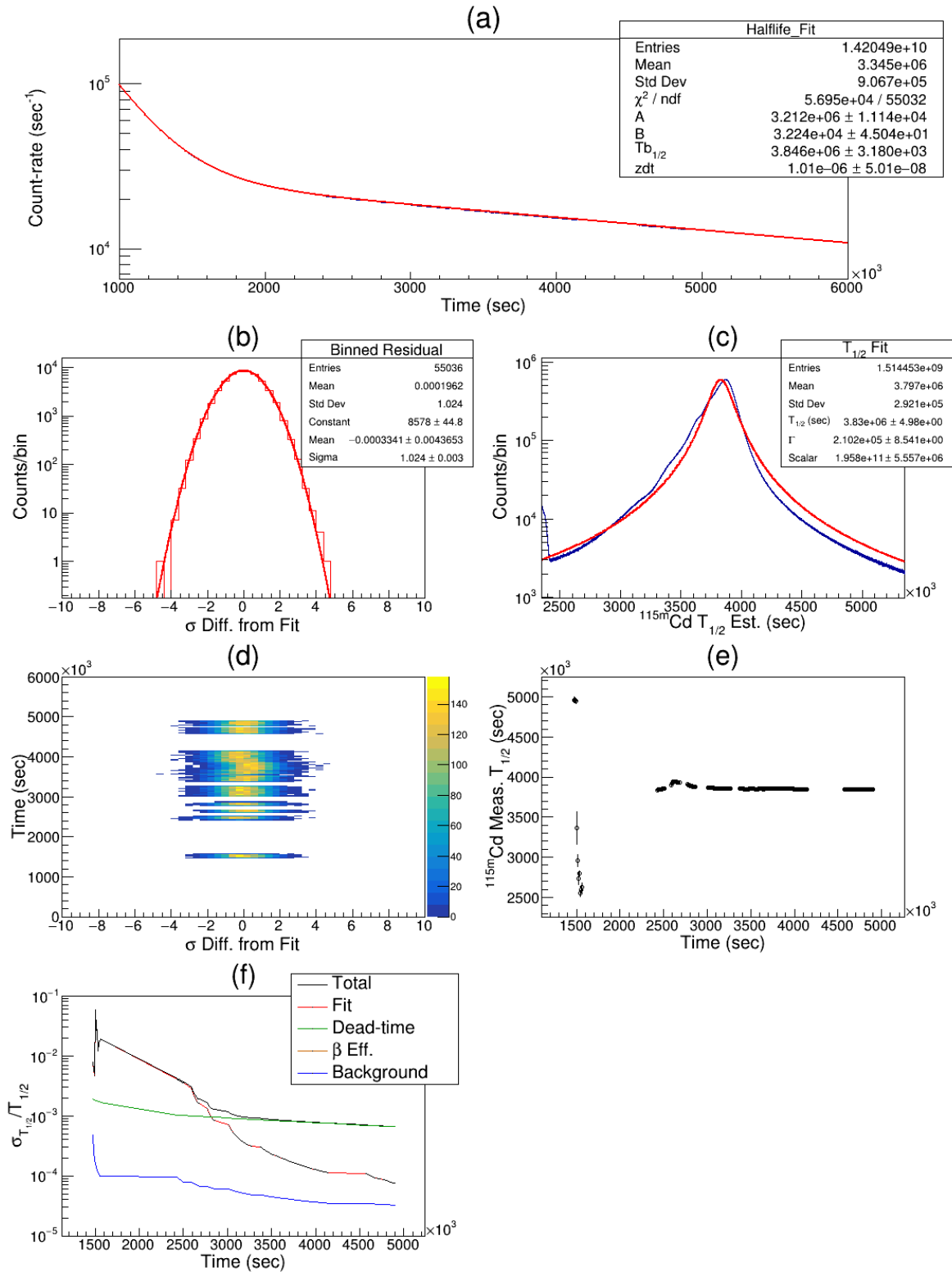In addition to measurements made using the Gaby instrument. The activity of the sample was also tracked using conventional singles gamma spectroscopy, high-efficiency liquid scintillation counting and gas proportional counting. The GEA1, GEA2, and LSC1 samples were counted over 136 days on 10 different detectors 22 times at distances of 19 cm from the detector face and later 7 cm as the sample activity began to compete with background. Initial measurements of the activity of ^{115m}Cd by gamma and by beta using LSC and gas proportional counting illustrate the significant discrepancy between these two methods of quantification as shown in Table 3-5.

It is important to note, that the LSC and gas proportional counters were calibrated using Sr/Y-90 standards corresponding to a 546 keV and 2279 keV endpoint beta energies, respectively. As such, the true beta efficiency for ^{115m}Cd is expected to be slightly lower with an endpoint energy of 1620 keV. The ^{115m}Cd specific-activities determined by all three instruments are summarized in Table 3-5.

Table 3-5. Summary of GABY3 massic activity by beta for LSC, gas proportional, and GABY instruments.

Instrument	kBq/g	StDev	RSD
LSC	32.24	0.04	0.124%
GAB, 1601	32.80	0.10	0.305%
Gaby, LSC (ε_β~100%)	32.24	0.05	0.155%
Gaby, LSC-g (934 keV γ gate, ε_β~95.1%)	33.86	0.05	0.148%
GEA**	19.85	6.94(0.22&)	1.15%
**Using NNDC Branching Ratios (Blachot, Oct. 2012) &Standard deviation of 22 measurements conducted over 140 days			

Most decay pathways for ^{115m}Cd result in the emission of multiple gammas from the same parent decay. The time between these gamma emissions depends on the lifetime of the excited state in the daughter nucleus, which is typically much shorter than the timing resolution of HPGe detectors (with the notable exception of the 336 keV level with a half-life of 4.486(4) hrs). As a result, a single HPGe detector is unable to distinguish multiple coincident emissions which may result in summing in or summing out of the full energy photo-peak. This process can be accounted for by either correcting using Cascade Summing Correction (CSC) factors or by increasing the standoff between the source and the detector to minimize the cascade summing occurring. Conventionally, branching ratios are determined using detectors placed at sufficient standoffs to minimize these cascade summing effects, which greatly increases the measurement time required to reach desired uncertainty targets.

We have developed an alternative approach, in which branching ratios can be determined without neglecting cascade summing corrections by iteratively solving the problem using Monte-Carlo radiation transport modeling. This was accomplished using the PNNL developed G4CSC (Geant4 Cascade Summing Corrections) code package (Pierson, Hagen, & Archambault, G4CSC, 2022). The NNDC published branching ratios were used as a starting seed for the iterative optimization. G4CSC simulations were performed to calculate the CSC factors for every gamma line with stated intensity greater than 0.0018%, and subsequently the massic activity was determined for each gamma-line. The residuals for each gamma-line were calculated assuming a targeted massic activity of 32.24(5) kB/g and then branching ratios were adjusted in the Photon Evaporation (relative photon emission probabilities) and Radioactive

Decay (probability of feeding each level) datasets contained within the G4RadioactiveDecay module of Geant4 (Agostinelli, 2003). New CSC factors were then re-calculated, and the process was repeated until the massic activity determined by each gamma-line was within their expected measurement uncertainty.
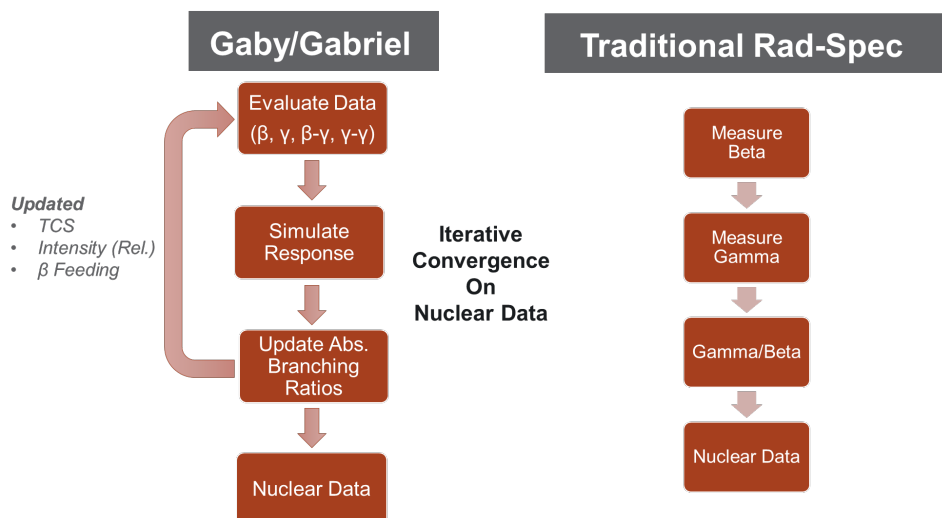

Figure 3-9. Branching ratio determination methodology for Gaby/Gabriel.

Figure 3-9 illustrates the two methods used to estimate the decay branching ratios of ^{115m}Cd. In the case of the Gaby instrument, the sample is located 1 mm from the detector face. In this counting geometry, coincident gamma-rays may strike the detector simultaneously removing both events from the measured spectrum. Such effects require calculated corrections to account for true-coincidence summing losses. However, the close counting geometry of the Gaby instrument allows for more accurate tracking of the decay rate of the sample for a much longer period producing more accurate half-life estimates and more data for monitoring the measured gamma-lines as further verification that they are not impacted by interferences.

In this experiment, traditional measurement techniques were used to generate independent estimates of the decay branching ratios using counting methods that virtually eliminated true-coincidence summing effects. As discussed earlier three independent fractions of the original solution were counted 22 times at distances of 19 cm from the detector face and later 7 cm. The standard deviation of the measured peak areas corrected for radioactive decay and detection efficiency were normalized by the measured sample activity by LSC to produce the branching ratio estimates presented in Table 4-1. Though these measurements do not include true-coincidence summing effects, the large stand-off distance of the sample to the detector significantly reduced the detection sensitivity of the instrument to weak gamma-lines that were observed in the Gaby and Gabriel instruments.

4.0 Results & Discussion

Table 4-1 contains estimates of the [115mCd] branching ratios using the advanced and conventional radiation detection systems at PNNL and Table 4-2 provides both current and historical context for the importance of these results. Early releases of the decay branching ratio data for this isotope were precise but extremely inaccurate, later evaluations reduced the precision with which the branching ratios were reported. The authors of this report suspect that differences in opinion between nuclear data evaluators at different times may have produced this variability. The uncertainty in the activity of the source in (Sergeev, Becker, Eriksson, Gidefeldt, & Holmberg, 1973) is likely the culprit of this error. Sergeev et. al. reported relative branching ratios and provided an estimate of the source activity but made no claim to present absolute branching ratios. However, evaluators may have discussed the precision and accuracy of the estimated activity presented in their paper to derive absolute branching ratios. Unfortunately, this error seems to have promulgated a bias between beta and gamma-ray activity estimates.

Table 4-1, Comparison of gamma emissions, branching ratios and associated uncertainties collected from GABY, conventional gamma spectroscopy and Gabriel.

	Gaby			Conventional			Gabriel		
Energy	Intensity	StdDev	RSD (%)	Intensity	StdDev	RSD (%)	Intensity	StdDev	RSD (%)
933.84	1.293	0.011	0.882	1.232	0.014	1.145	1.284	0.028	2.154
1290.59	0.566	0.005	0.938	0.534	0.008	1.498	0.574	0.011	1.992
484.47	0.194	0.002	0.786	0.187	0.004	2.139	0.181	0.003	1.627
1132.57	0.0535	0.0006	1.120	0.0514	0.0024	4.71	0.0548	0.002	3.059
158.03	0.0133	0.0002	1.578	0.0126	0.0015	11.9	0.0125	0.0003	2.469
1448.78	0.01047	0.00021	1.988	0.0098	0.0006	5.208	0.01068	0.00079	7.401
492.35				0.0081	0.0028	34.6	0.00565	0.00021	3.806
336.24							0.00353	0.00026	7.246
105.2	0.00266	0.00022	8.289				0.00337	0.00031	9.182
316.2	0.00389	0.00039	9.981				0.0034	0.0003	9.449
1418.24	0.000621	0.000016	2.600				0.000504	0.000029	5.675

Table 4-2, Comparison of current NNDC gamma-ray branching ratio estimates and uncertainties to the historic Firestone reference.

	NuDat 3 (2012)			Firestone, Table of Isotopes, 8th Ed., 1999 Update		
Energy	Intensity	StdDev	RSD (%)	Intensity	StdDev	RSD (%)
933.84	2	0.7	35.000	2.00	0.006	1.6%
1290.59	0.9	0.3	33.333	0.890	0.014	6.9%
484.47	0.29	0.1	34.483	0.290	0.020	1.2%
1132.57	0.09	0.03	33.333	0.0856	0.0010	
158.03	0.017	0.006	35.294	0.01702	0.00018	
1448.78	0.017	0.006	35.294	0.017	0.002	1.1%

5.0 Conclusion

We have demonstrated a new approach to perform precision measurements of gamma ray branching ratios of long-lived fission products and applied it to the study of β decays of ^{115m}Cd. The measurements of the WSU-PNNL made ^{115m}Cd samples led to new gamma ray branching ratios with 0.8% to 10% relative precision for absolute branching ratios spanning from 1.28% to 0.0005%, respectively. These branching ratios are a significant departure from the those stated in the most recent ENSDF evaluation done in 2012. Importantly, although the corrections to the primary gamma lines at 934 keV and 1291 keV are -36% and -37% respectively, they are nearly in line with the stated 1 sigma uncertainties of 35% and 33% given in the ENSDF evaluation.

Two approaches were used to produce mono-isotopic sources of ^{115m}Cd. The first made use of the ^{115}In(n,p)$^{115m/g}$Cd proton knockout threshold reaction induced by a Thermo-Scientific accelerator driven deuterium-tritium fusion neutron source. The second used thermal neutron capture on an isotopically enriched ^{114}Cd target. Pros and cons of each approach are listed below in Section 6.0.

6.0 Future Work

The path for irradiations is dependent on what is needed for the exercise, there are drawbacks and benefits to each path. Below is a discussion of several the salient points for a 14 MeV neutron irradiation and a thermal neutron irradiation.

- **14 MeV Neutron Irradiation of In**

    - Relies on a lower probability nuclear reaction, an n,p reaction on ^{114}In.

    - Requires separation to remove the In, though with the established methods for separation a 99.99+% pure $^{115m/g}$Cd source

    - Produces a pure $^{115m/g}$Cd with no stable Cd or other Cd isotopes

    - Lower neutron flux (1×10^9 n/cm^{2}s)

    - Can be made in individual batches for each lab

    - ^{115}In is the predominant In isotope.

    - Production of ^{115m}Cd ~10 times more relative to ^{115g}Cd for ^{115}In(n,p) reaction relative to thermal neutron capture on ^{114}Cd

    - Chemistry is required, In activation will occur at >10 fold higher rate than n,p reaction. Therefore, activated In must be removed

    - Chemical separation is relatively simple

    - Chemistry can occur within 30 minutes after irradiation

    - Indium metal or Indium oxide can be easily dissolved

- **Thermal Neutron Irradiation**

    - High probability nuclear reaction n,γ on ^{114}Cd

    - Requires enriched ^{114}Cd

        - 98% ^{114}Cd is available from the National Isotope Development Center

        - PNNL material contained various other isotopes including ^{108}Cd

    - Significantly higher neutron flux using WSU TRIGA reactor or another

    - Can model irradiation after 2nd PNNL irradiation

        - Irradiate 8+ hours each day for 7 days, with the residual ~16 hours being used to decay the ^{115}Cd

- Can be used to counter the lower ^{115m}Cd production rate from thermal relative to 14 MeV

o Lower production of ^{115m}Cd relative to ^{115}Cd.

o Can make significant activity that can be split between all possible participants

o Cd metal is easily dissolved

o Contains significant quantity of stable Cd, from unactivated ^{114}Cd or other stable Cd in the metal.

o Chemistry is not necessary but can purify the Cd

7.0 References

Agostinelli, S. (2003). Geant4 - A Simulation Toolkit. *Nucl. Instrum. Meth. A, 506*, 250-303.

Blachot, J. (Oct. 2012). Nuclear Data Sheets for A = 115. *Nuclear Data Sheets*, vol. 113, no. 10, pp. 2391–2535.

Brun, R., & Rademakers, F. (1997). ROOT—an object oriented data analysis framework. *NIM-A*, vol. 389, iss. 1, pg. 81-86.

Martell, A. E., Smith, R., & Motekaitis, R. (2004). NIST Standar Reference Database 46: NIST Critically Selected Stability Constants of Metal Complexes Databases (Version 8.0). . College Station, Texas, USA.

Mougeot, X. (2019). BetaShape code (INDC(NDS)---0783). *International Atomic Energy Agency (IAEA)*.

Pierson, B., & Archambault, B. (2022, January 22). *TListSpectrum*, 0.1a. Retrieved from TListSpectrum - A custom toolkit for analysis of list-mode data: https://gitlab.pnnl.gov/areas/tlistspectrum

Pierson, B., Hagen, A., & Archambault, B. (2022, January 22). *G4CSC*, 0.1a. Retrieved from G4CSC - Geant4 Cascade Summing Corrections: https://gitlab.pnnl.gov/ares/g4csc

Rademakers, F., & Brun, R. (1997). ROOT - An Object Oriented Data Analysis Framework. *Nucl. Inst. & Meth. in Phys. Res. A, 389*, 81-86.

Sergeev, V., Becker, J., Eriksson, L., Gidefeldt, L., & Holmberg, L. (1973). Levels in 115In populated in the decay of 115mCd. *Nuclear Physics A*, vol. 202, iss. 2, pg. 385-395.

Pacific Northwest National Laboratory